



Chapter 2

Experimental Section

This chapter II contains a comprehensive description of the procedure of preparation of different sample used in our research work along with various techniques used for the characterization and investigation of material.

2.1 Sample preparation

The first step of experimental physics/material investigation is always sample preparation. A good quality (pure phase) of samples is indispensable for the experimental characterization and analysis of the inherent physical properties of the material which can be easily compare with the different existing theoretical models. A poor quality (with impurity phase) of samples will may give complicated results owing to the different stimuli like distortion, defect, off-stoichiometry etc. However, sometime presence of impurity phase gives some surprising result, for example emergence of superconductivity in $\text{La}[\text{O}_{1-x}\text{F}_x]\text{FeAs}$ [124]. The double perovskites and pyrochlore oxides, which is presented in the earlier chapter are ceramic material by nature. Almost all the oxides, which is used as a starting material for synthetizations of these oxides, have high melting temperature and does not react at low temperature, thus cannot be simply deposited or melted similar to intermetallic compounds. Hence, they are prepared usually through solid-state synthetic route [125] which is discussed below.

2.1.1 Solid state reaction method

This method is an important synthetic route widely used in fabrication of many solid inorganic polycrystalline samples from a stoichiometric mixture of starting materials. In this method the reactions among the starting materials start only at high temperatures (1000 to 1500 °C) and it may take several days to form a single desired phase. For example, Fig. 2.1 is

demonstrating the mechanism, steps and physical appearance of a typical solid-state reaction for formation of $A_2B_2O_6$ using AO and BO_2 starting material [AO (solid) + BO_2 (solid) \rightarrow $A_2B_2O_6$ (solid)]. At certain high temperature the reaction can start at the boundaries of AO and BO_2 crystals and forms a $A_2B_2O_6$ product layer. The initial stage of the reaction forms the nuclei of $A_2B_2O_6$ crystallites adjacent to their interface. The nucleation of $A_2B_2O_6$ is very

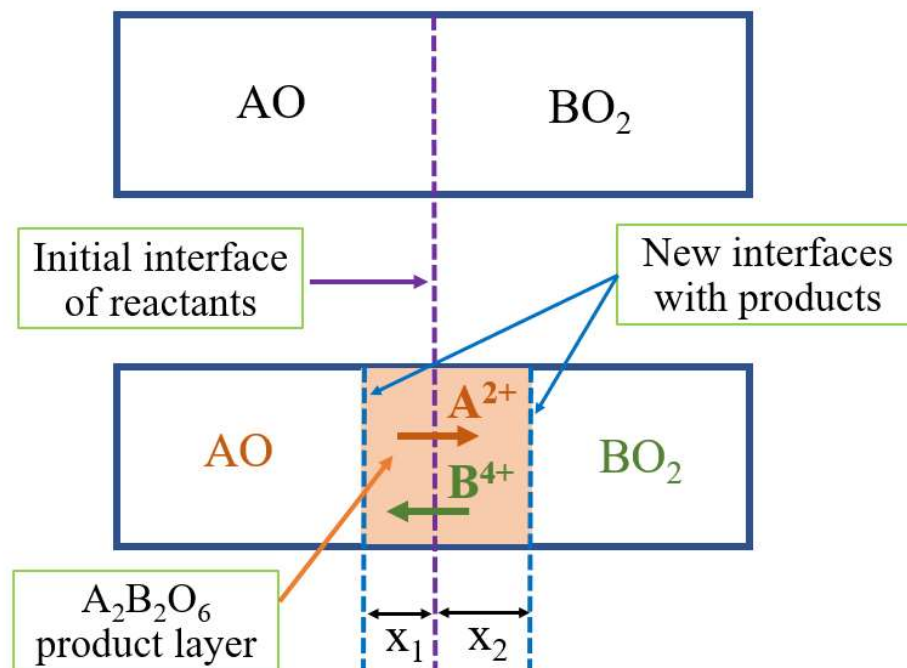


Figure 2.1: Showing schematic mechanism of the solid-state reaction.

difficult as they are different than the starting reactants with different structure. Thus, the nucleation of desired product needs structural rearrangement as well as breaking of the A-O & B-O bonds of the reactant, discharging, diffusing and relocation of A^{2+} and B^{4+} ions on the lattice points. This process can be realized only at high temperatures depending on reaction conditions like surface area, structure, reactivity of reactants and the thermodynamic free energy change during the reaction. Also, the growing of nucleus is difficult as A^{2+} and B^{4+} ions

from the reactants need to diffuse through two boundaries. Nevertheless, the diffusion of A^{2+} and B^{4+} ions is favored by increase in temperature which leads to the growth of product layer. However, the rate of the reaction diminishes on the thickening of product layer. As we know the diffusion of ions is mainly driven by their concentration gradient. At the certain temperature, the diffusion rate decreases owing to the thickening of the product layer and the smoothing of the concentration gradient. At this stage, we need to create fresh reaction surface through regrinding of the reacted mixture to acquire effectiveness of the material preparation.

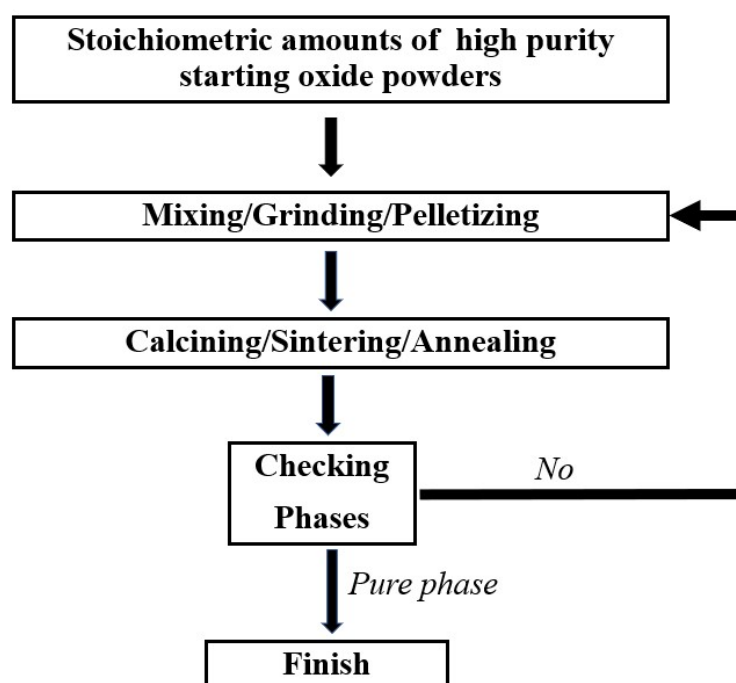


Figure 2.2: A typical flow chart of sample synthesis using solid state reaction.

Throughout this research work, the solid-state reaction route has been used for the sample preparation, where the stoichiometry amount of highly pure oxide powders was taken according to desire product and ground for an hour in an agate mortar. This mixture was subjected initial heat treatment for a few days (calcination) at a lower temperature (1000-1100^o

C) for pre-reaction and nucleation of the product phase using a muffle furnace in air. After cooling this reaction mixture was reground and put at several higher temperatures for several days (1150-1250⁰ C) with intermittent grindings for further reaction and growth of product nuclei (this is step is known as sintering). The phase was analyzed repeatedly during the sintering process using the powder X-ray diffraction (XRD) measurements. Numerous cycles sintering processes followed by grinding are required to attain the desire phase. For the instance, when we detect a pure phase using the XRD, the sintered powder were pressed into the pellets, under the ~5 MPa pressure by means of the hydraulic press, and placed at some higher temperature (1300-1350⁰ C) for a few days for final sintering. These sintered pellets were used to explore their different physical properties for example, structural, electrical, magnetic, optic, spectroscopic, etc. The generalized process of solid-state reaction route is shown in Fig. 2.2 using flow chart and more details of starting materials and reaction condition are described in coming chapters.

2.2 Sample characterization

2.2.1 X-ray diffraction technique

The “X-ray diffraction (XRD)” technique is furthermost essential, non-destructive procedures to examine the phase and crystal structure of the any crystalline/polycrystalline materials qualitatively as well as quantitatively. As the many physical properties of materials (specially, electrical, magnetic and optical) are correlated with the arrangement of atoms/ions/molecules on their crystallographic sites, thus the structural information turn out to be necessary for the investigation of materials, hence measurement of X-ray diffraction

spectrum becomes essential. The basic concept of XRD can be understood by well-known Bragg's relation, i.e.

$$2d_{hkl} \sin \theta = n\lambda \quad (2.1)$$

Where, λ = wavelength of the X-rays radiation which is used for diffraction, d_{hkl} = Interplanar separation of planes of Miller indices (hkl), θ = angle between incident/diffracted beam and corresponding lattice plane, and n = Integers, used to represent the order of diffraction and it is usually unity in our study. When the incident radiation satisfies the Bragg's law, the diffracted beam will make coherent superposition and a maximum intensity can be recorded using a detector.

Actually, a crystal behaves as 3-dimensional diffraction gratings with spacing similar to the atomic planes of the crystal lattice. Interestingly, the wavelength of the X-ray radiation is also of the order of interplanar distances ($\sim 1 \text{ \AA}$) of the crystalline materials. Thus, the X-rays will be scattered from crystalline solid and will produce diffraction pattern by constructive interference. In our study, a collimated monochromatic beam of X-ray radiation from X-ray tube with a copper source ($\text{Cu-K}\alpha = 1.5418 \text{ \AA}$) attacks on the powdered sample and get diffracted. The diffracted beam is collected using a moveable detector (for example scintillation counter, Geiger counter or image plate). The intensity of the diffracted beam as a function of the incident angle is called "diffraction pattern". The analysis of the diffraction pattern of any sample, using Rietveld method provides the detailed crystallographic information. The diffractometer used in our study, i. e. the Rigaku-Miniflex II DESKTOP X-ray diffractometer working at 30 kV and 15 mA, is shown in Fig. 2.4.

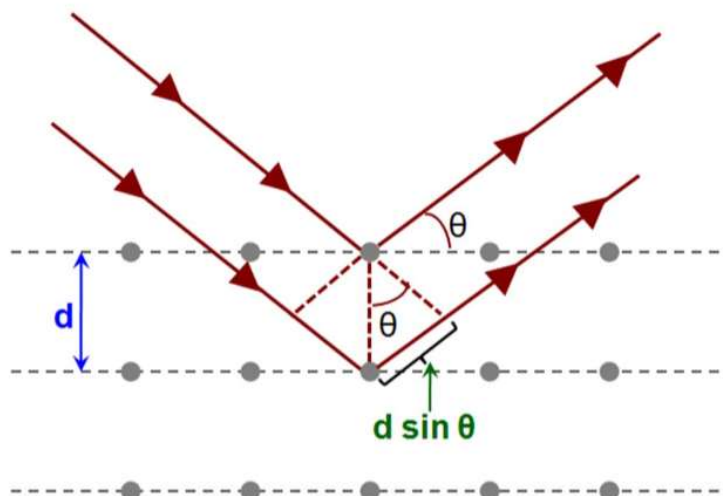


Figure 2.3: Demonstrating Bragg's law [https://dictionary.iucr.org/Main_Page].

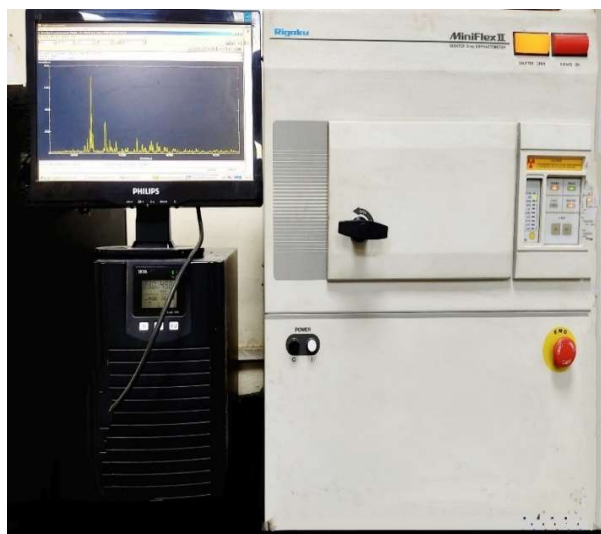


Figure 2.4: Rigaku-MiniFlex-II DESKTOP powder X-ray diffractometer set up.

2.2.2 Magnetization measurement and MPMS

The magnetization measurements in our study have been performed using Quantum Design Magnetic Property Measurement system, i.e., “MPMS3” (see Fig. 2.5 (a)). The MPMS3 magnetometer allows magnetization measurement in the temperature range 1.8 K to 400 K using the ^4He based cryostat and magnetic field range ± 7.0 Tesla with several choice of measurements. This magnetometer has a very high sensitivity ($\sim 10^{-8}$ emu) with a user-friendly operating system.

The heart of MPMS is the Superconducting Quantum Interference Device (SQUID) sensor having two parallel Josephson Junctions, where two superconductors are separated by two thin insulating (weak link) layers (see Fig. 2.5 (b)). The SQUID working principle was given by B. D. Josephson theoretically in 1962. According to this effect, a current is builds (known as supercurrent) with a maximum critical value I_C and flows continuously through the weak link without any voltage across the Josephson junction via tunnelling of Cooper pairs. Since the SQUID has a superconducting ring, thus it allows only a magnetic flux through it whose magnitude is the integral multiple $\Phi_0 = h/2e = 2.07 \times 10^{-15}$ Tesla-m² (which is the flux quantization in superconductor). For any change in magnetic flux through the loop, a screening current will be induced in superconducting ring to maintained flux quantization. The small magnitude of Φ_0 allows to develop an extremely sensitive magnetic sensor like SQUID. Using SQUIDs, the magnetic flux related to any materials can be converted to voltage, owing to the flux quantization sensitivity in superconductors. The external biased current through the SQUID instigates the electron Cooper pairs to tunnel through the weak link junctions. When an external magnetic field of any material enters in the ring, it changes the critical current

through the superconductor. This change in current is amplified to voltage signal using electronic instruments which is calibrated to give the magnetic moment of system. Henceforth, the SQUID also known as flux-to-voltage transducer and it can transform a tremendously minor change of magnetic flux to a voltage signal.

As mentioned earlier, “MPMS3” magnetometer have been used for magnetization measurements in our work. This system provides three possible mode of magnetization measurements: (i) DC scan mode (ii) AC susceptibility mode and (iii) VSM (vibrating sample mode). We have used vibrating sample mode in our investigation. This mode is described by Faraday’s law of electro-magnetic induction, which says that changing electric field through any circuit will bring a magnetic field in the system as well as changing magnetic field will yield an electric field. While operating in vibrating sample mode the material (which is to be investigated) is put in a uniform external magnetic field and subsequently the sample get magnetized due to the aligning of the magnetic dipole in the direction of the applied field and the net magnetic moment increases with increase in externally applied field. The moment of magnetic dipoles induces an additional field (known as stray field) near the sample. This additional induce field will change with time when the material vibrates up and down. The change in the magnetic field will be sensed by a set of highly sensitive SQUID based pick up coils. According to Faraday’s law, this changing magnetic field will produce an electric field and consequently an induced current proportional to the magnetization of the material. This induced current signal is amplified using different electrical amplifier and has been monitored by a computer using various software. Finally, the signal is converted to corresponding magnetic moment of the sample under investigation using the computer, which is calibrated with some standard sample.

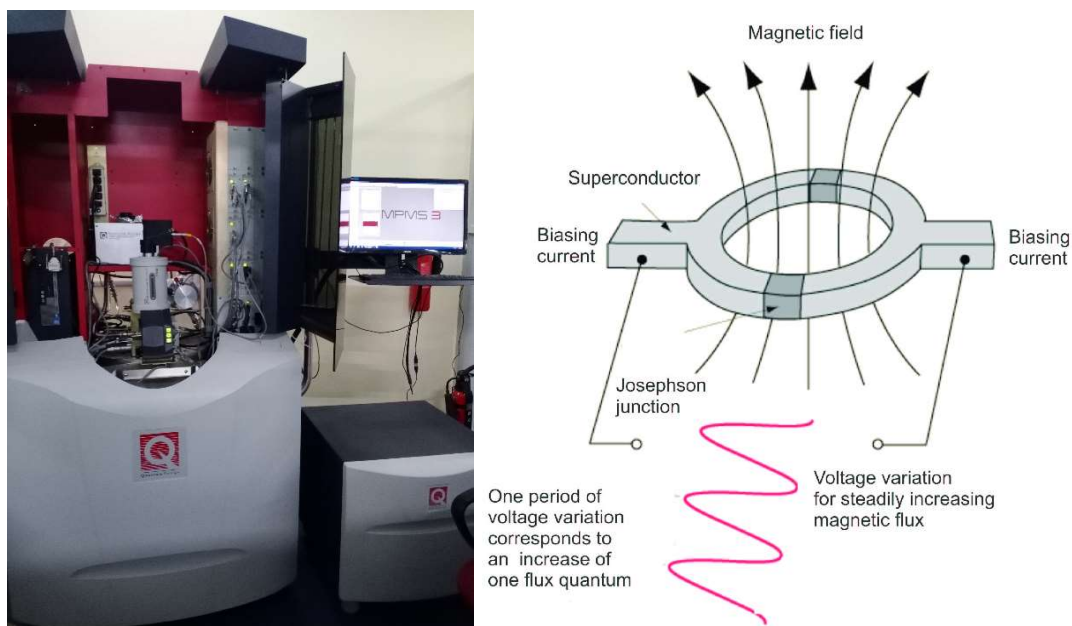


Figure 2.5: (a) Picture of the Quantum Design MPMS3 situated in the CIFC of our institute (b) Shows the schematic view of a SQUID sensor.

2.2.3 X-ray photoemission spectroscopy

The “X-ray photoemission spectroscopy (XPS)” has been broadly used for the identification elemental composition, oxidation state/electronic structure & their dynamics in atoms, and ligand co-ordination, which is required for explanation of different physical/chemical properties of samples. This is also used to identify the active sites, surface contamination or dust on the sample, oxide layers on non-oxide materials, etc. The XPS is surface sensitive technique and it gives the information of elements present at/near (20 to 50 Å below the surface) the surface of materials [6].

The basic concept at the XPS technique is based on the concept of Einstein’s photoelectric effect. Here, a monochromatic beam of photons (X-ray) is irradiated on the surface of the compound, and a secondary beam of electrons is ejected by absorbing these

photons from the materials. This ejected beam of electrons is analysed, thus XPS is a type of electron spectroscopy and also known as ESCA (electron spectroscopy for chemical analysis).

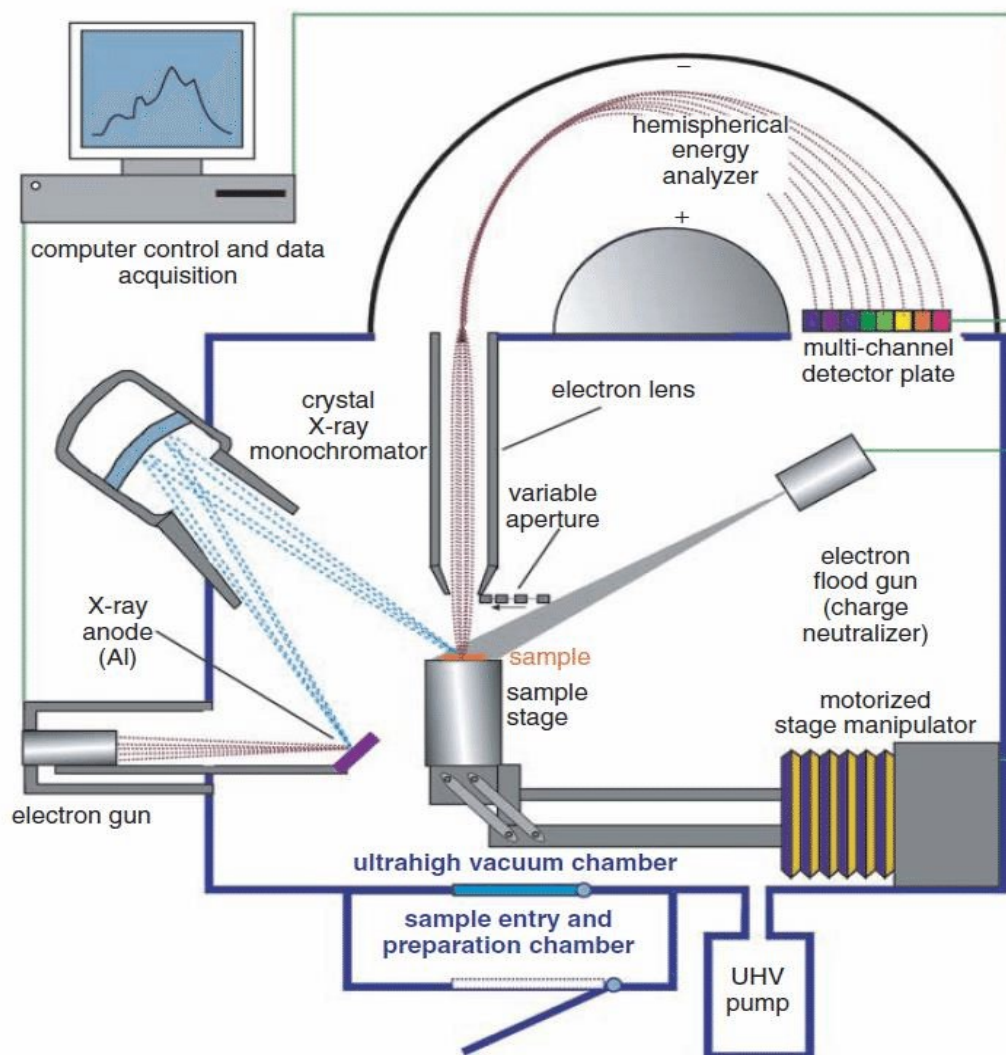


Figure 2.6: The schematic diagram of the XPS instrumentation.

If a photon of energy $h\nu$ fall on the surface of the sample and an electron from the inner shell gets ejected by absorbing this photon then the kinetic energy (K.E.) of this electron, detected at the analyzing unit of XPS instrument is given by,

$$\text{K.E.} = h\nu - \text{B.E.} - \Phi \quad (2.2)$$

Where, B.E. is the binding energy of the ejected electrons and Φ is the work function of spectrometer of instrument. As the K. E. of ejected core electron is function of binding energy and thus a characteristic of the element present in material and the XPS spectra are designed as variation of number of ejected electrons as a function of B.E. A schematic diagram of XPS measurement is illustrated in Fig. 2.6. The various components of XPS are listed as,

i) Source: The photon source in XPS is usually X-ray radiation from an Aluminum or magnesium target. A monochromator is used to reduce the band width of X-ray photons, which provides a very small spot on the sample surface.

ii) Sample holder: Here sample (to be examine) is placed which lies between the entrance slit of spectrometer and source. The zone around the sample holder is kept at ultrahigh vacuum ($\sim 10^{-5}$).

iii) Analyzer: The analyzer is hemispherical in shape and kept in a very high static electric field. The electrons entering into the analyzer follows a curved route with curvature depending on the strength of the electric field and their K.E.

iv) Detector: Its place where the electrons are multiplied and converted into a pulse of electrons.

v) Signal processor and read out: This unit amplifies the signals and converts it into a spectrum.

2.2.4 Raman spectroscopy

The “Raman spectroscopy” is based on the scattering of light through a matter. Historically, after the discovery of Compton scattering in 1923, where X-ray is scattered by

electrons and the wavelength of the X-ray is changed, C. V. Raman thought the optical analogue of Compton effect and ultimately in 1928, Raman with his research partner Krishan was able to discover the Raman spectroscopy. When Raman did his first, he used sunlight as a source and his naked eye as a detector, due to unavailability of advanced instrumentation. Afterwards, the light was allowed to fall on a photographic plate. Later on, a lot of improvements have been made like invention of a good excitation source with advanced detector and a commercial Raman spectrometer was accessible. And this spectroscopy become an innovating technique to probe the qualitative and quantitative dynamic of atoms/ions/molecules in crystal using the scattering of light. While light scattering from the molecule/crystal, the most of photons get elastically scattered. The elastically scattered photons will possess the same energy as the incident photons. There is a very small fraction of light (~ 1 photon out of 10^7 photons) which gets inelastically scattered with a change in their wavelengths by changing by changing rotational/vibrational/electronic energy of the molecule. This inelastic scattering is known as the famous Raman Effect (i.e., usually described as Raman shift) and the elastic scattering is recognized as Rayleigh scattering.

The phenomena of Raman effect can be explained based on the deformation of molecules in an electric field of strength E owing to the induced electric dipole moment, $P = \alpha E$ (α is the polarizability). The Raman shift can be observed only the derivative of α is non-zero with respect to Q (normal co-ordinates). When electromagnetic radiation interacts with the atom/molecule the electron clouds and bonds of the molecules get distorted. Due to this interaction, the atom/molecule get excited to a virtual energy state from their ground state thus becomes unstable. These excited molecules returns to a different stable state (rotational or vibrational) by decreasing their energy through releasing a photon. The difference in energy of

initial stable state of and final stable of the molecule cause shifting of the frequency of the emitted photon from the excitation energy. If the final state has large energy, then the we get a emitted photon of a lower frequency than the excitation frequency and this shifting of energy

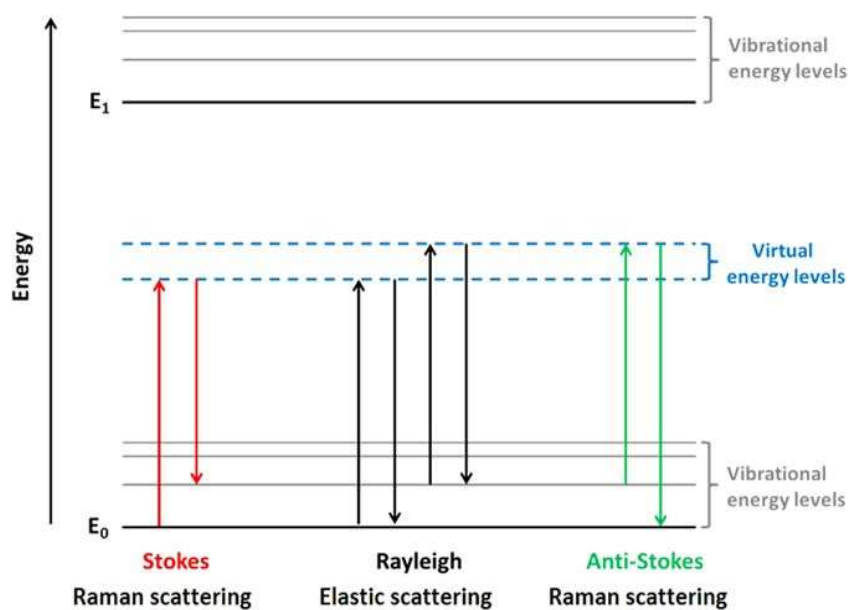


Figure 2.7: Illustration of Raman effect using energy level diagram.



Figure 2.8: Showing the picture of Renishaw micro-Raman spectroscope used in our characterization.

of scattered photon is known as stoke shift (Fig. 2.7). However, when the final state has lesser energy then we get a emitted photon higher energy and this shifting is nominated as Anti-Stokes shift. The Raman spectra are usually described in terms of wave numbers in the units of inverse of length (cm^{-1}).

In our study, we have used Reinshaw Raman spectrometer, which is shown in Figure 2.8. Here, a monochromatic laser light of wavelength 532 nm, using diode-pumped solid state laser with a maximum power of 100 milli Watt was used. To avoid heating of the specimen, only 5% power was allowed to incident on the sample. The laser beam was focus at a much shorter working distance over a $50\times$ long-distance objective connected with the Leica DM 2500M microscope. A dispersion grating with 2400 groves/mm with 50 micron slit width has been used to keep the constant phase throughout the experiments. The scattered light has been collected and passed to a detector. The data was collected using the supplied 4.0 software Spectrometer scanning and finally processing of data was finished.

2.2.5 UV-Vis (Ultraviolet-Visible) spectroscopy

The “ultraviolet-visible spectroscopy” is a typical absorption/reflectance spectroscopy in the ultraviolet-visible region of electromagnetic spectrum. This spectroscopy has been extensively used to study of the light absorbing capacity of a material as well as to estimate the optical band gap of that material When the UV-Vis light of intensity I_o passes through the sample and the intensity of transmitted light comes out to be I then the ratio I/I_o is defined as the transmittance (T). In terms of percentage T expressed as,

$$\%T = [I/I_o] \times 100 \quad (2.3)$$

From the transmittance value one can estimate the amount of light absorbed i. e. absorbance (A) in terms of transmittance (T) using the relation,

$$A = -\log(T/100) \quad (2.4)$$

This spectroscopy can also be used to examine the reflectance of any material. In this purpose, we measure the intensity of reflected light from that sample (I) using UV-Vis spectrometer, and it is compared with the reflected light intensity (I_0) of a reference material. Then the ratio I/I_0 is referred as reflectance of the sample.

The UV-Vis spectrophotometer a diffraction grating is used which work as monochromator and separates the dissimilar wavelengths of incident light by collecting the lights of several wavelengths. The usual radiation source used are usually a Tungsten filament (300 nm to 2500 nm), a deuterium arc lamp (190 nm to 400 nm), and now a days people are using Xenon arc lamps and light emitting diodes (LEDs) for the visible lights. The detector used in this spectrometer are a charged couple device or a photodiode. In our study we have the Lambda-35 UV-vis spectrophotometer from Perkin Elmer for the UV-visible absorption measurement.



Figure 2.9: UV-Visible spectrometer set up.

2.2.6 Transport property measurement

The resistivity of the samples under investigation have been estimated using electrical resistance measurement of that sample. We have measured the resistivity of our sample by means of Keithley 6517B electrometer, which is used for measuring a high resistivity (from 225 kilo-Ohm to 2 giga-Ohm). The temperature of the sample was changed and controlled using a He-based CCR (closed cycle refrigerator) and a Cryocon 32B temperature-controller. The sample used for this purpose was pellets with a circular cross-section of ~ 5 mm radius and few mm (1-2 mm) width. The both circular faces of the pellets were coated with silver paste which work as a metal electrode plate along with two thin copper wires attached at same face. This prepared sample is then mounted in the CCR chamber and the electrometer was connected with the copper wires attached with sample. The CCR chamber was put in a high vacuum using a rotary vane vacuum pump. And finally, the resistivity was measured at different temperatures. Moreover, the resistivity was also measured under application of magnetic field using an electromagnet up to 1.2 Tesla.

2.2.7 Dielectric spectroscopy

The dielectric measurement is a very important experimental method for the characterization of the semiconducting/insulating sample to prove different interesting phenomena like dipolar relaxation, dipolar ordering, ferroelectricity as well as electric conduction. In dielectric study we estimate the relative electrical permittivity (ϵ_r) i. e. dielectric constant of the materials. The relative electrical permittivity is complex quantity and thus expressed in real (ϵ_r') and imaginary parts (ϵ_r'') i.e., $\epsilon_r = \epsilon_r' + i\epsilon_r''$ of the electrical permittivity. The ϵ_r' represent the total energy stored due to polarization in every cycle whereas ϵ_r''

represent the energy loss per cycle. These quantities may change depending on the various parameters like temperature, pressure, frequency, electric and magnetic fields, etc.

In our research study we have estimated the dielectric constant from the capacitance measurement (as described in chapter 1) using a Keysight E4980A Precision LCR meter, which is a famous impedance analyzer for the dielectric spectroscopy with a high precision and sensitivity. Here, the sample is put in the middle of two metallic electrodes, forming a parallel-plate capacitor type arrangement. Then the, the sample is biased with an alternating voltage signal $V_s(f)$ and with an alternating current $I_s(f)$ using the LCR meter. At the same time the impedance (Z) of the sample is calculated using the Ohm's law, $Z = V(f)/I(f)$. This impedance is connected with the capacitance (C) of the sample as, $C = -i/2\pi fZ$, where $i = \sqrt{-1}$ (the imaginary factor) and f is the frequency of the alternating signals. A He-cooled closed cycle refrigerator (CCR) and Cryocon 32B temperature controller was used to control the temperature of the sample as described in section 2.2.6.

